FY-14 FCRD Milestone: M3FT-14OR0202232 FCRD Advanced Fuels Campaign (AFC) Level 3 Milestone Report

Letter Report Documenting Progress of Second Generation ATF FeCrAl Alloy Fabrication

Y. Yamamoto, Y. Yang, K.G. Field, K. Terrani, B.A. Pint, and L.L. Snead Oak Ridge National Laboratory

Abstract

Development of the 2nd generation ATF FeCrAl alloy has been initiated, and a candidate alloy was selected for trial tube fabrication through hot-extrusion and gun-drilling processes. Four alloys based on Fe-13Cr-4.5Al-0.15Y in weight percent were newly cast with minor alloying additions of Mo, Si, Nb, and C to promote solid-solution and second-phase precipitate strengthening. The alloy compositions were selected with guidance from computational thermodynamic tools. The lab-scale heats of ~ 600g were arc-melted and drop-cast, homogenized, hot-forged and -rolled, and then annealed producing plate shape samples. An alloy with Mo and Nb additions (C35MN) processed at 800°C exhibits very fine sub-grain structure with the sub-grain size of 1-3µm which exhibited more than 25% better yield and tensile strengths together with decent ductility compared to the other FeCrAl alloys at room temperature. It was found that the Nb addition was key to improving thermal stability of the fine sub-grain structure. Optimally, grains of less than 30 microns are desired, with grains up to and order of magnitude in desired produced through Nb addition. Scale-up effort of the C35MN alloy was made in collaboration with a commercial cast company who has a capability of vacuum induction melting. A 39lb columnar ingot with ~81mm diameter and ~305mm height (with hottop) was commercially cast, homogenized, hot-extruded, and annealed providing 10mm-diameter bar-shape samples with the fine sub-grain structure. This commercial heat proved consistent with materials produced at ORNL at the lab-scale. Tubes and end caps were machined from the bar sample and provided to another work package for the ATF-1 irradiation campaign in the milestone M3FT-14OR0202251.

1. Introduction

The development of nuclear-grade *enhanced accident tolerant fuel* FeCrAl alloys at Oak Ridge National Laboratory (ORNL) has been initiated targeting new, iron-base structural alloys for nuclear fuel cladding, substituting for zirconium alloys. The aim is to produce clad exhibiting improved mechanical properties over a wide temperature range with oxidation and irradiation resistance under normal and transient operating conditions. The FeCrAl family of alloys were selected based on their excellent oxidation resistance in high temperature steam environments up to 1475°C (provided by the sufficient amounts of Cr and Al additions), compared to the industry standard zirconium alloys which are problematic above 900°C [1-4]. Significant reduction in oxidation kinetics, along with associated reduction in hydrogen production, is one of the major routes to enabling enhanced accident tolerant fuels and reactor cores. Moreover, with the superior high temperature strength compared to zirconium alloys, utilization of this class of alloys is expected to enhance burst margins during design basis accident scenarios and

potentially for conditions extending beyond those limits. It is noted that a significant consideration in the application any Fe-based alloys is the neutron impact, leading to the desired thinning of the Fe-ally clad wall as compared to typical zircaloy alloy. The thinning of the alloy and associated reduction in neutronic impact may ultimately be a trade-off with any improved mechanical property gained (i.e. while the steel is mechanically superior, by thinning the wall this benefit may be diluted for the sake of increased neutron performance.) The current alloy design strategy is focused on developing a nuclear-grade material that exhibits comparable or superior behavior under normal operating conditions (at 320°C in pressurized water reactor environments) when compared with today's commercial Zr-based alloys. Once this step is accomplished on the laboratory scale, a commercial-base processing route for thin-wall tube production will be developed to enable deployment of this class of alloys as nuclear fuel cladding.

The present work package consists of two phases. In Phase I, the ORNL FeCrAl model alloys were prepared for distribution in order to evaluate the various material properties as a function of Cr and Al levels. The main purpose was to find out the composition dependence of basic properties such as fabricability, tensile property, oxidation resistance, weldability, irradiation resistance, and so on, and then downselect one or more candidate alloy composition(s) as a basis with promising oxidation resistance at elevated temperatures. This phase II focuses on optimizing mechanical properties to meet or exceed the minimum requirements from the strategy of "fuel cladding materials with accident tolerance". Phase I was completed in FY13 and resulted in downselction of a candidate base alloy composition of "Fe-13Cr-4.5Al-0.15Y" in weight percent [5,6]. Phase II was initiated in the latter part of FY13 and a multi-faceted program continues.

The objective of this milestone report is to document the progress of the optimization efforts in Phase II, specifically focused on improvement of the mechanical performance of the nuclear-grade FeCrAl alloys for LWR fuel cladding with enhanced accident tolerance. The base alloy composition of Fe-13Cr-4.5Al-0.15Y, selected in Phase I, exhibited the balanced properties of a good oxidation resistance [7] with minimally acceptable levels of Cr and Al levels such that impacts of irradiation embrittlement, formability, and issus related to high ductile-brittle-transition-temperature (DBTT) are minimized [8-11]. The development of the Phase II alloys, or so-called "2nd generation ATF FeCrAl alloys", has been conducted by applying minor alloying additions of Mo, Si, Nb, and C to the base alloy composition in order to promote solid-solution strengthening and second-phase precipitate strengthening, with guidance from computational thermodynamic tools. One candidate alloy was selected for trial tube fabrication study with a scale-up effort through a commercial casting company. The machined tubes and end caps made of the candidate alloy were provided to another work package for the ATF-1 irradiation campaign in the milestone M3FT-14OR0202251.

2. Experimental procedure

Phase equilibrium of the model alloys was initially calculated by using thermodynamic software "OCTANT" and "JMatPro® (version 6) with Fe database". Alloy compositions were selected based on the calculation with the design strategy of applying solid-solution strengthening and

second-phase precipitate strengthening. The lab-scale heats were cast at ORNL by using arcmelting in a back-filled argon gas atmosphere with pure element feedstock and/or pre-alloyed Al-Y to make ~ 600 g button ingots. The ingots were flipped and melted several times to avoid any potential ingot inhomogeneity. Ingots were then drop-cast in a back-filled argon gas atmosphere to a water-cooled copper mold with a size of $25 \times 25 \times 75$ mm to make bar-shape castings. An commercially-produced alloy (C35MN5) was cast by Sophisticated Alloys, Inc. through a vacuum induction melting as a larger scale round billit, of 81 mm diameter and 305 mm height. **Table I** summarizes the analyzed chemistry of the alloys in as-cast status. Note that T35Y2 is a 1st generation FeCrAl alloy used as a reference material, which was cast by Sophisticated Alloys, Inc. and then hot-extruded at ORNL.

Table I: Nominal and analyzed alloy compositions of the ORNL ATF FeCrAl alloys studied

Name		Fe	Cr	Al	Υ	Мо	Si	Nb	С
T35Y2	Nominal	82.35	13	4.5	0.15	-	-	-	-
	Analyzed	82.26	13.15	4.44	0.12	<0.01	0.01	<0.01	0.002
C35M	Nominal	80.15	13	4.5	0.15	2	0.2	-	-
	Analyzed	80.88	12.68	4.22	0.031	1.92	0.20	<0.01	0.003
C35MC	Nominal	80.07	13	4.5	0.15	2	0.20	-	0.08
	Analyzed	80.96	12.53	4.22	0.026	1.94	0.21	<0.01	0.089
00514110	Nominal	79.83	13	4.5	0.15	2	0.20	0.3	0.02
C35MNC	Analyzed	80.41	12.77	4.31	0.065	1.95	0.20	0.24	0.026
COEMAN	Nominal	79.15	13	4.5	0.15	2	0.20	1	-
C35MN	Analyzed	79.96	12.77	4.22	0.032	1.94	0.21	0.81	0.004
C35MN5	Nominal	78.53	13	5.2	0.07	2	0.20	1	-
	Analyzed	78.68	13.02	5.08	0.032	1.99	0.21	0.97	0.003

All alloys were homogenized at 1200°C in Ar gas. The lab-scale heats were hot-forged at 1200 or 800°C to make disk-shape samples with ~8mm thickness, rolled to make plate-shape samples with ~0.89mm thickness (total more than 90% thickness reduction), and then annealed at the same temperature for up to 24h for recrystallization and grain size control. T35Y2 and C35MN5 were extruded at ORNL at 1050 and 800°C, respectively, and then annealed at 700 and 800°C, respectively. In order to control the microstructure of C35MN5, more than 97% of total area reduction was applied which was achieved by conducting the extrusion twice. Microstructure was characterized by using a light optical microscope and a scanning electron microscope (SEM) with back-scattered electron (BSE) mode. SEM- electron backscatter diffraction technique was used for crystallographic analysis of the obtained grain structure.

Dog-bone shaped sub-size tensile specimens (SS-3, in **Figure 1**) were machined from the plate-shape samples. The specimens were used for tensile testing over a temperature range from room temperature to 800°C. The hot-extruded bar specimens were machined to make a tube shape with 9.37mm \pm 0.025mm outer diameter, 0.52mm \pm 0.013mm wall thickness, and 75.6 mm \pm 0.025mm length, together with a pair of end caps to seal the tube by using welding, as shown in **Figure 2**.

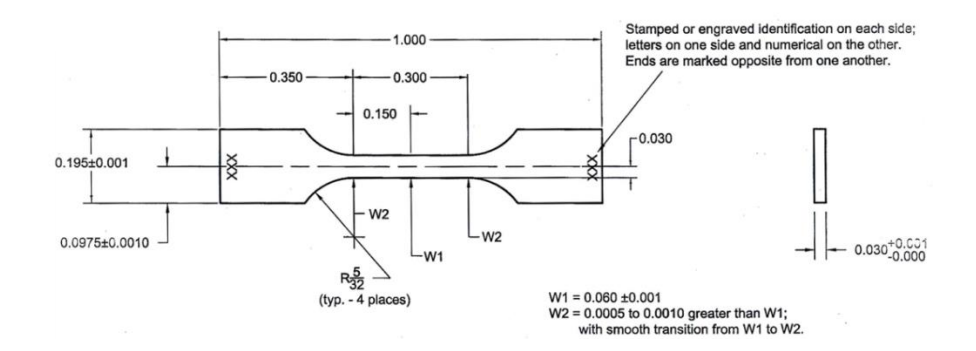


Figure 1. Drawings of dog-bone shape sub-size tensile specimens (SS-3).

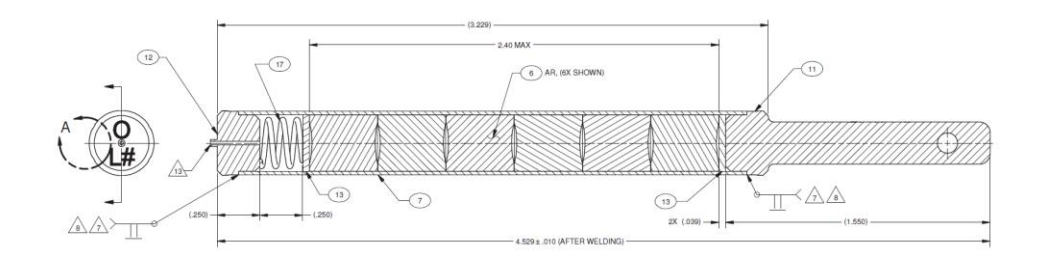


Figure 2. Schematic illustration of the assemble of a tube and end caps to be machined from the extruded FeCrAl bar. Note that the fuel pellets and the spring will not be provided from the current milestone.

3. Results and discussion

Prediction of phase equilibrium

Thermodynamic calculation predicted several different second-phase formations which potentially act as strengthening precipitates in the 2^{nd} generation ATF FeCrAl alloys. **Figure 3** shows the calculated phase equilibrium of the Fe-13Cr-4Al-2Mo-0.2Si with or without Nb and C, as a function of temperature. Note that Y is not available in the database, so that the results were from the alloys without Y. C35M expected only a solid-solution strengthening from the Mo addition, but Fe₂(Mo,Nb) Laves phase would form below 640°C as a byproduct. C35MC showed Cr-rich carbides ($M_{23}C_6$ and M_7C_3) over almost the entire temperature range that could be attributed to the very low carbon solubility in the ferrite matrix. C35MNC showed NbC instead of Cr-rich carbides in C35MC because of strong C stabilizing effect of Nb. C35MN exhibited more Laves formation than the others which would form up to 1000°C. All alloy compositions were selected to show complete solid solution range at elevated temperature, in order to control the second-phase precipitate dispersions though the heat treatment. It should be emphasized that the temperature range of α -Cr formation is insensitive to the minor alloying additions in the

range studied, indicating that the effect of alloying additions on the potential embitterment at \sim 320°C due to α -Cr formation can be considered as negligibly small in this study.

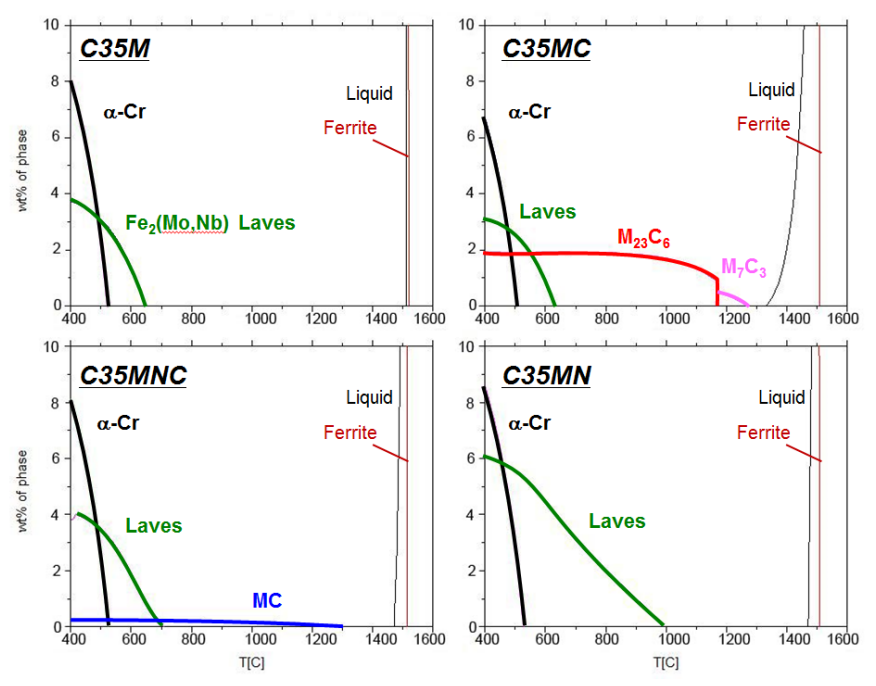


Figure 3. A calculation result of the phase equilibrium of Fe-13Cr-4Al-2Mo-0.2Si base alloys with or without additions of Nb and C.

Microstructure characterization

Minor alloying additions are considered for refining the grain size compared to the reference alloy. **Figure 4** summarizes the microstructure of the 2nd generation ATF FeCrAl alloys (C35~) processed at 800 and 1200°C, compared with the 1st generation FeCrAl model alloy (T35Y2) containing no minor alloying additions. The alloys processed at 1200°C showed fully recrystallized microstructure with more than 100µm grain size, with a few Y-rich precipitate dispersions. No second-phases were observed, as, for the most part, predicted from the calculation. C35M processed at 800°C showed uniform grain size in a range from 30-50µm which was smaller than that of the T35Y2 processed even at lower annealing temperature, indicating that the Mo addition could retard the recrystallization kinetics, C35MC and C35MNC were annealed for 24h at 800°C in order to obtain fully recrystallized microstructure, and resulting grain sizes were ~100µm with relatively elongated grains along the rolling direction (parallel to the horizontal direction in the pictures). C35MN did not show recrystallization even after 24h annealing at 800°C. Figure 5 shows SEM-BSE images of the 2nd generation ATF FeCrAl alloys processed at 800°C. The predicted second-phases such as M₂₃C₆, MC, and Laves were observed in the alloys. Note that the size of M₂₃C₆ was more than 10µm which would not contribute the strengthening at all. C35MN also exhibited very fine grain size microstructure with ~1-3µm grain sizes, together with dispersion of sub-micron size Laves phase precipitates on the grain boundary. SEM-EBSD analysis indicated that they were sub-grain structure, as described in the latter part of this report.

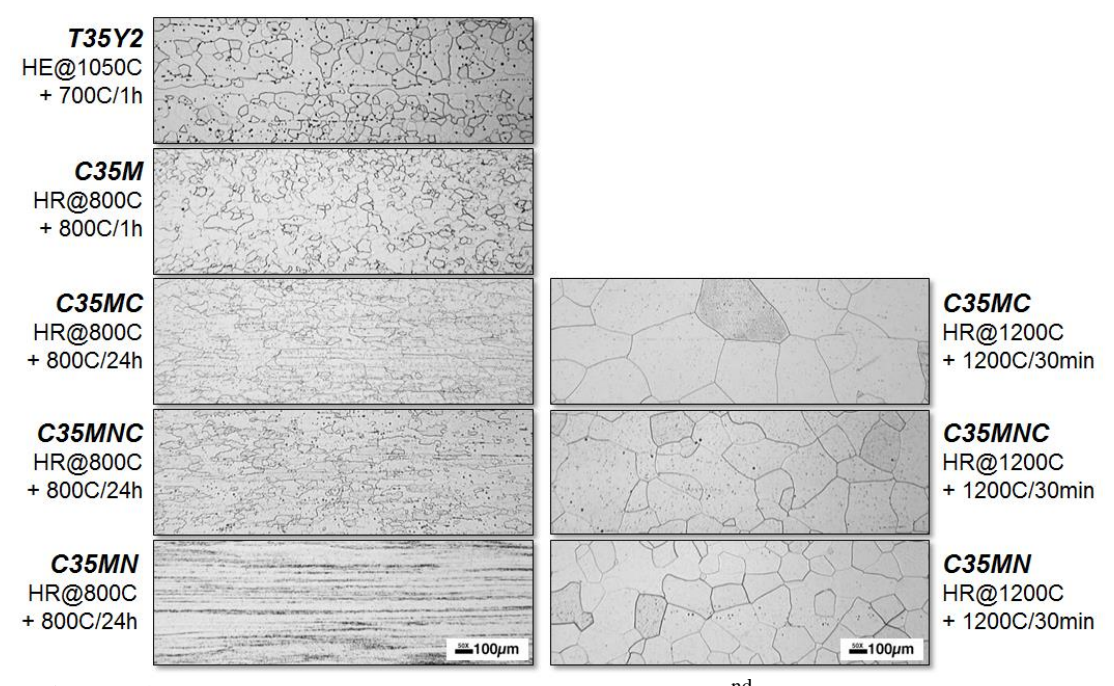


Figure 4. Light optical micrographs showing the 2nd generation ATF FeCrAl alloys processed at 800 (left-hand side) and 1200°C (right-hand side).

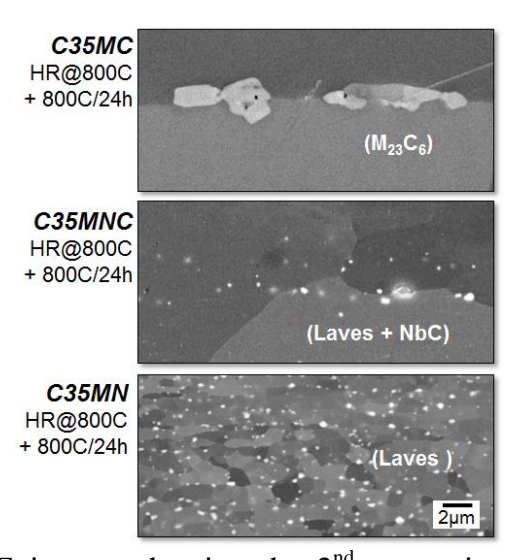


Figure 5. SEM-BSE images showing the 2^{nd} generation ATF FeCrAl alloys processed at 800° C.

Tensile properties

Tensile properties of the 2nd generation ATF FeCrAl alloys (C35~), corresponding to the materials shown in Figure 4, are summarized in **Table II**. The results of T35Y2 are also shown for comparison purpose. Only slight improvement of the properties in C35M, C35MC, and C35MNC processed at 800°C were observed compared to T35Y2, indicating that the expected

solid-solution strengthening or precipitate strengthening are not significant in the case of fully recrystallized microstructure tested at room temperature. On the other hand, the C35MN processed at 800°C showed more than 25% improvement of the yield and tensile strengths together with decent ductility. The properties of C35MC, C35MNC and C35MN processed at 1200C showed slightly improved properties compared with the 800°C-processed alloys even with the larger grain sizes, indicating that dissolution of minor alloying elements (C and/or Nb) contributed the solid-solution strengthening. However, the very fine grain size in the 800C-processed C35MN seemed more effective for improving the tensile properties drastically.

Table II: Room temperature tensile properties of the 2nd generation ATF FeCrAl alloys.

Nome	Downsules	Dragon	CC	at room temperature			
Name Remarks		Process	GS, um	YS, MPa	TS, MPa	UL, %	TL, %
T35Y2	model alloy	HE1050C + Ann 700C-1h-WQ	50-80	384	536	21.8	37.5
C35M	Mo + Si	HR800C + Ann 800C-1h-WQ	30-50	451	570	17.9	33.9
C35MC	Mo+Si+C	HR800C + Ann 800C-24h-WQ	<100	412	549	14.3	23.0
C35MNC	Mo+Si+Nb+C	HR800C + Ann 800C-24h-WQ	<100	448	592	15.8	27.1
C35MN	Mo+Si+Nb	HR800C + Ann 800C-24h-WQ	~1	629	811	12.0	21.6
C35MC	Mo+Si+C	HR1200C+ Ann 1200C-1h-WQ	300-500	589	633	1.7	3.9
C35MNC	Mo+Si+Nb+C	HR1200C+ Ann 1200C-1h-WQ	100-300	445	562	16.3	27.6
C35MN	Mo+Si+Nb	HR1200C+ Ann 1200C-1h-WQ	100-300	566	662	7.6	14.1

The Nb addition was the key to maintain the fine sub-grain microstructure in C35MN at elevated temperature. Figure 6 shows the microstructure of C35M processed and annealed at 650°C. The sub-grain structure similar to the 800C-processed C35MN can be obtained by selecting the lower processing temperature, although there was no Laves phase formation in the microstructure because of the absence of Nb addition in the alloy. After 24h annealing at 650°C, the alloy started to show partial recrystallization, and it was fully recrystallized after 168h annealing. This was not the case for the C35MN processed and annealed at 800°C, indicating that the Nb addition was somehow playing an important role to increase the thermal stability of the sub-grain structure, such as grain boundary pinning effect from the Laves phase precipitates. Table III shows the room temperature properties of the C35M alloy with sub-grain structure, partially recrystallized microstructure, and fully recrystallized microstructure. The sub-grain structure showed the highest yield and tensile properties similar to the C35MN, and the strengths decreased with proceeding recrystallization. These results indicated that the microstructure (or grain size) control would be more dominant factor to control the tensile properties among these alloys, and the minor alloying additions can be used not for the direct strengthening species but for the supportive elements of the microstructure evolution and its stability.

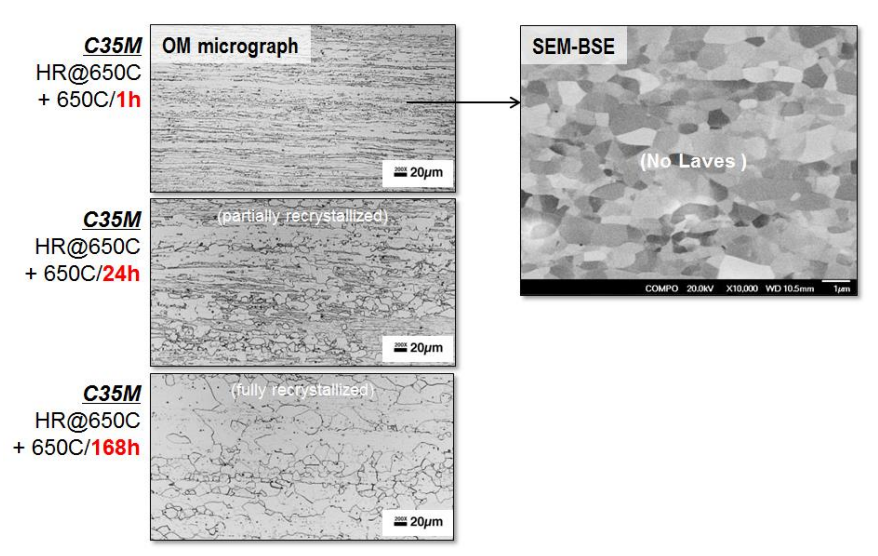


Figure 6. Light optical micrographs and a SEM-BSE image showing the C35M alloy processed and annealed at 650°C.

Table III: Room temperature tensile properties of the C35M alloy with different microstructure.

Name	Process	Microstructure	at room temperature				
Name	Process	Microstructure	YS, MPa TS, MPa		UL, %	TL, %	
C35M	HR650C + Ann 650C-1h-WQ	Sub-grain structure	674	756	10	19	
C35M	HR650C + Ann 650C-24h-WQ	Partially recrystallized	572	696	17	27	
C35M	HR800C + Ann 800C-1h-WQ	Fully recrystallized	451	570	17.9	33.9	
C35MN	HR800C + Ann 800C-24h-WQ	Sub-grain structure	629	811	12.0	21.6	

Scale-up efforts of C35MN alloy and tube fabrication

The C35MN alloy was selected for the trial tube fabrication study. In order to obtain the bar shape samples with ~10mm diameter as well as the sub-grain structure for the improved strength, a large ingot with more than 70mm in diameter was procured from a commercial cast company. The heat ID was "C35MN5" which was cast by using vacuum induction melting, containing a little higher Al than C35MN to expect a better oxidation resistance. The cast ingot was sectioned into several pieces, homogenized at 1200°C for 2h, and then machined the diameter to fit with the sleeve of the extrusion press. **Figure 7** summarized the procedure of the extrusion process as listed below;

- (1) Soaked at 800°C/1.5h + extruded from 74mm to 35mm in diameter + water-quenched
- (2) Machined 32mm diameter x 127mm length, and then inserted into 1018 steel cans with 74mm outer diameter
- (3) Soaked at 800°C/1.5h + extruded from 74mm to 29mm in diameter + water-quenched
- (4) Annealed at 800°C/1h + water-quenched



Figure 7. Hot-extrusion process of the C35MN5 alloy to make 10mm-diameter bar samples.

The as-extruded microstructure is shown in **Figure 8**. The SEM-BSE image shows the sub-grain structure with dispersion of Laves phase precipitates, similar to that of C35MN shown in Figure 5. The SEM-EBSD analysis revealed that the crystallographic misorientations between the grains aligned parallel to the rolling direction (horizontal axis of the image) were less than 15°, indicating that they consisted of sub-grains. Further detailed characterization by using transmission electron microscope is currently in progress. The extruded C35MN5 were machined into tubes and end caps as shown in **Figure 9**, and they were provided for the ATF-1 irradiation campaign in the milestone M3FT-14OR0202251.

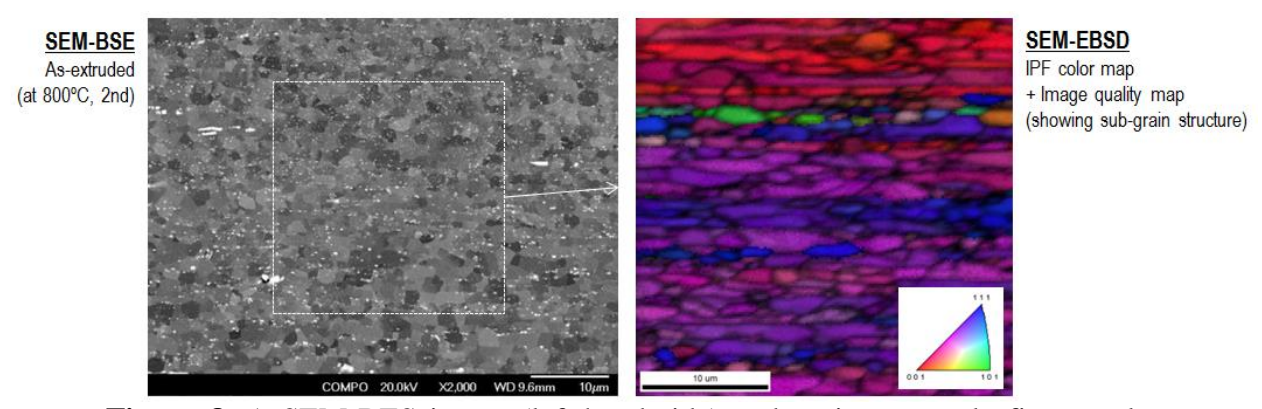


Figure 8. A SEM-BES image (left-hand side) and an inverse pole figure color map overlapped with image quality map obtained from SEM-EBSD analysis (right-hand side) of the as-extruded C35MN5 alloy.



Figure 9. Machined tube and end caps for ATF-1 irradiation campaign.

5. Summary and future development activity

Development and evaluation of the 2^{nd} generation ATF FeCrAl alloy has been initiated. Four alloys based on Fe-13Cr-4.5Al-0.15Y in weight percent were newly cast with minor alloying additions of Mo, Si, Nb, and C to promote solid-solution strengthening and second-phase precipitate strengthening. The lab-scale heats with ~ 600g were arc-melted and drop-cast, homogenized, hot-forged and -rolled, and then annealed producing plate shape samples. An alloy with the Mo and Nb additions (C35MN) processed at 800°C showed a very fine sub-grain structure with the sub-grain size of 1-3 μ m which exhibited more than 25% better yield and tensile strengths together with decent ductility compared to the other FeCrAl alloys at room temperature. It was found that the Nb addition was the key to improving thermal stability of the fine sub-grain structure.

Scale-up effort of the C35MN alloy was successfully made in collaboration with a commercial cast company who has a capability of vacuum induction melting. A 39lb columnar ingot with ~81mm diameter and ~305mm height (with hot-top) was commercially cast, homogenized, hot-extruded, and annealed providing 10mm-diameter bar-shape samples with the fine sub-grain structure. This commercial heat proved consistent with materials produced at ORNL at the lab-scale. Tubes and end caps were machined from the bar sample and provided to another work package for the ATF-1 irradiation campaign in the milestone M3FT-14OR0202251.

Further detailed characterization and property evaluation at elevated temperatures are currently in progress. Another tube fabrication effort through a commercial tube-drawing company has been initiated by using the C35MN5 alloy. Oxidation test results of various 2nd generation ATF FeCrAl alloys will be updated in the milestone report M3FT-14OR0202231.

6. Acknowledgements

The authors would like to acknowledge Dr. Lizhen Tan for his review and helpful comments on this report, and Ms. Mary Snead for her administrative support. This research was funded by the

U.S. Department of Energy's Office of Nuclear Energy, Advanced Fuel Campaign of the Fuel Cycle R&D program.

7. References

- [1] Powers, D.; Meyer, R. Cladding swelling and rupture models for LOCA analysis, NUREG-0630; U. S. Nuclear Regulatory Commission: 1980.
- [2] B.A. Pint, K.A. Terrani, M.P. Brady, T. Cheng, J.R. Keiser, Journal of Nuclear Materials in press (2013).
- [3] M. Moalem, D.R. Olander, Journal of Nuclear Materials 182 (1991) 170.
- [4] K. Suzuki, S. Jitsukawa, N. Okubo, F. Takada, J.Nucl.Eng. and Design 240 (2010) 1290–1305.
- [5] Y. Yamamoto et al., FY13 FCRD milestone report, M2FT-13OR0202291 (2013).
- [6] B.A. Pint, FY13 FCRD milestone report, M2FT-13OR0202132 (2013).
- [7] Stott, F.; Wood, G.; Stringer, J., The influence of alloying elements on the development and maintenance of protective scales. *Oxidation of Metals* **1995**, *44* (1-2), 113-145.
- [8] Courtnall, M.; Pickering, F., The effect of alloying on 485 C embrittlement. *Metal Science* **1976**, *10* (8), 273-276.
- [9] Mathon, M.; De Carlan, Y.; Geoffroy, G.; Averty, X.; Alamo, A.; De Novion, C., A SANS investigation of the irradiation-enhanced α–α' phases separation in 7–12 Cr martensitic steels. *Journal of nuclear materials* **2003**, *312* (2), 236-248.
- [10] Qu, H.; Lang, Y.; Yao, C.; Chen, H.; Yang, C., The effect of heat treatment on recrystallized microstructure, precipitation and ductility of hot-rolled Fe-Cr-Al-REM ferritic stainless steel sheets. *Materials Science and Engineering: A* **2013**, *562*, 9-16.
- [11] Field, K.G.; Gussev, M.N.; Yamamoto, Y.; Snead, L.L., Deformation behavior of laser welds in high temperature oxidation resistant Fe-Cr-Al alloys for fuel cladding applications, *Journal of nuclear materials*, Accepted for publication **2014**.